Austin Journal of Radiology

Open Access

Austin Publishing Group

Research Article

Comparison of FDG and FLT PET/CT Imaging Based on Human Non-Small Cell Lung Carcinoma Tumor Size in a Small Animal Model

Choi EK[1#], Jung HY[2#], Yoo IR[1*], Chung YA[1], Park SI[2] and Maeng LS[2]

[1]Department of radiology, College of Medicine, The Catholic University of Korea, Seoul, Republic of Korea

[2]Institute of Catholic Integrative Medicine (ICIM), Incheon St. Mary's Hospital, The Catholic University of Korea, Seoul, Republic of Korea

***Corresponding author:** Yoo IR, Department of Radiology, Seoul St. Mary's Hospital, College of Medicine, The Catholic University of Korea, 222, Banpo-daero, Seocho-gu, Seoul, South Korea

[#]Choi EK and Jung HY contributed equally to this work.

Received: August 26, 2016; **Accepted:** October 06, 2016; **Published:** October 12, 2016

Abstract

Our goal was to investigate FDG and FLT uptake based on tumor size and the correlation with Ki-67 staining in an Non-Small Cell Lung Carcinoma (NSCLC) xenograft model. A549 human NSCLC cells were subcutaneously implanted into the flanks of nine nude rats. Standardized Uptake Value (SUV) parameters were obtained from FDG and FLT PET/CT images, including SUVmax, SUVmean, tumor to Non-Tumor Ratio (TNR), and Coefficient Of Variation (COV). SUVmax was higher in FDG PET than in FLT PET imaging (P=0.039). Significant correlations of tumor size with SUVmax, TNR, and COV were observed in FDG imaging (r=0.852, P=0.004; r=0.676, P=0.046; r=0.817, P=0.007), but no such correlations were found in FLT imaging (r=0.195, P=0.615; r=0.419, P=0.261; r=0.117, P=0.764). There were significant correlations of the Ki-67 index with SUVmax, TNR, and COV in FLT imaging (r=0.866, P=0.003; r=0.745, P=0.021; r=0.721, P=0.029), but no such correlations in FDG imaging (r=0.478, P=0.193; r=0.478, P=0.193; r=0.617, P=0.077). Our data demonstrated that FDG uptake was better visualized in the tumor and correlated significantly better with tumor size compared with FLT in an NSCLC xenograft model. The tumor heterogeneity on FDG PET correlated well with tumor size, while no correlation was found for FLT.

Keywords: ^{18}F-FDG; ^{18}F-fluorothymidine; PET; Lung neoplasms

Introduction

Biological markers of tumor growth and proliferation have emerged as important prognostic factors in patients with Non-Small Cell Lung Carcinoma (NSCLC) [1]. The molecular characteristics obtained from measurement of tumor growth and proliferation related to DNA synthesis can be important factors for making treatment plan decisions and selecting optimized anticancer therapy at initial diagnosis. In addition, imaging plays a role in risk stratification and prognosis prediction. Many previous studies have established predictive tools for evaluating the biologic processes affecting tumor growth and aggressiveness [2,3].

Functional imaging techniques such as Positron Emission Tomography (PET) can be useful to obtain information on the biological features of the tumor such as biomarkers of metabolism, proliferation, and hypoxia [4-6]. Fluorodeoxyglucose (FDG) is a widely used radiopharmaceutical that allows assessment of tumor cellular glucose utilization, and the use of FDG PET for the detection, staging, therapeutic response evaluation, and prognosis prediction for NSCLC has been expanding [7-9]. However, FDG is selectively taken up by both tumor cells and inflammatory cells, which results in false-positive findings. To overcome this flaw, several PET tracers targeting proliferation and hypoxia of the tumor cell have been developed. In addition, new PET tracers for fatty acid, choline metabolism, amino acid transport, and protein synthesis have been introduced, although they are not yet widely available.

Attempts to assess the cellular proliferative activity have been made with several DNA precursors that are involved in the DNA replication phase [10,11]. Of the agents that target DNA synthesis, F-18 Fluorothymidine (FLT) has been widely exploited in clinical oncology because of its favorable metabolic rate, optimal half-life, and commercial availability [12,13]. Compared with FDG, FLT shows higher discrimination between tumor and inflammatory cells and has fewer false-positive findings [14,15]. However, several studies have shown that the uptake of FLT is not clearly visualized and shows low sensitivity in NSCLC [16]. FLT uptake may vary based on Ki-67 expression, which binds to nuclear antigens expressed by cells in the G1, G2, M, and S proliferative phases [17]. Furthermore, whether the amount of FLT uptake depends on tumor size remains unclear, while studies have shown that the degree of FDG uptake correlates directly with tumor size [5]. This uncertainty may be due in part to tumor heterogeneity caused by differences in the tumor microenvironment and differences in proliferation, hypoxia, and necrosis [18,19]. To our knowledge, few studies have directly compared FDG and FLT imaging techniques with regard to tumor size. To understand the relationship between FDG and FLT uptake and tumor size, the correlation between FDG and FLT uptake by tumor size was evaluated in an NSCLC xenograft model. Therefore, the aim of our study was to compare FDG and FLT uptake according to tumor size and demonstrate the correlation with the proliferative activity in an NSCLC xenograft model.

Citation: Choi EK, Jung HY, Yoo IR, Chung YA, Park SI and Maeng LS. Comparison of FDG and FLT PET/CT Imaging Based on Human Non-Small Cell Lung Carcinoma Tumor Size in a Small Animal Model. Austin J Radiol. 2016; 3(4): 1058.

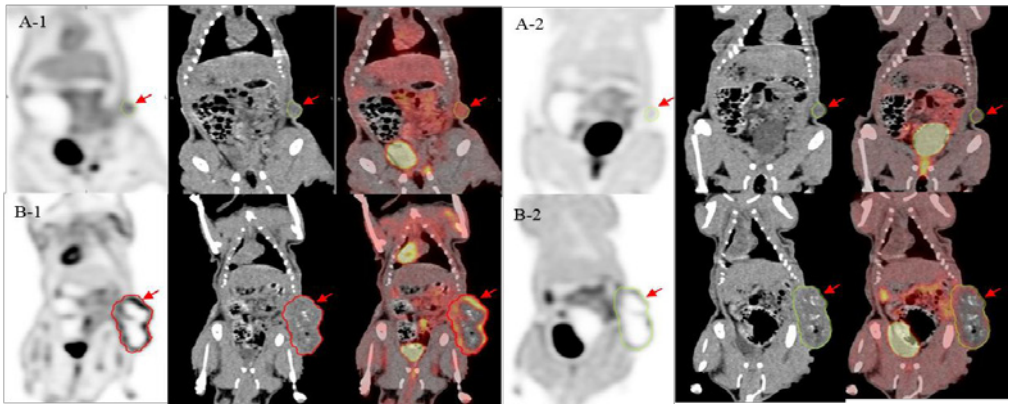

Figure 1: FDG and FLT PET/CT images of NSCLC at different tumor sizes. Radiotracer uptake is more discrete in in the FDG PET/CT images (A-1: SUVmax, 1.0; tumor to non-tumor ratio, 2; coefficient of variation, 0.3) than in FLT PET/CT images (A-2: SUVmax, 0.4; tumor to non-tumor ratio, 1; coefficient of variation, 0.3) in small-sized tumors. Similarly, FDG uptake is better visualized in FDG PET/CT images (B-1: SUVmax, 4.6; tumor to non-tumor ratio, 3.1; coefficient of variation, 0.6) than in FLT PET/CT images (B-2: SUVmax, 1.1; tumor to non-tumor ratio, 2.2; coefficient of variation, 0.4) in large-sized tumors.

Materials and Methods

Tumor cell culture

Human NSCLC A549 cells were obtained from American Type Culture Collection (Manassas, VA, USA, http://www.atcc.org) and maintained in Dulbecco's modified Eagle's medium (DMEM; Hyclone, Logan, UT, USA) including 10% heat-inactivated fetal bovine serum, 100 U/ml penicillin, and 100 μg/ml streptomycin. The cells were incubated at 37°C in a humidified atmosphere containing 5% CO_2.

Animal models

The experimental protocol was approved by the Institutional Animal Care and Use Committee of Catholic University Medical School, and all experiments were performed in accordance with our institutional guidelines. Six-week-old male athymic Crl: NIH-Foxn1^{rnu} rats (Charles River) were housed in an optimal temperature-, humidity-, and light-controlled environment. Food and water were freely available. For the tumor xenograft model, the rats were anesthetized with 5% isoflurane in 70% nitrous oxide and 30% oxygen using an induction chamber and maintained by a mixture of 2% isoflurane under temperature-controlled conditions (37°C ± 0.1°C). After receiving anesthesia, a single dose of 1×10^7 A549 tumor cells in 200 μl of DMEM was injected subcutaneously into the flank of the rats. After tumor implantation, the tumor diameter was measured daily with calipers to monitor growth. When the nodular lesion on the tumor implant site grew to >5 mm in gross diameter, it was selected for the PET/CT experiment. PET/CT imaging was performed on a different date for each rat to assess metabolic activity according to the tumor size.

PET using F-18 FDG and F-18 FLT

After the rats were anesthetized with intraperitoneal injection of ketamine (80 mg/kg) and xylazine (10 mg/kg), about 37 MBq (0.5 ml) of the radiotracer (either FDG or FLT) was injected intravenously via a lateral tail vein. After allowing the radiotracer to distribute for 1 h, the rats were anesthetized for the PET/CT scan. PET/CT images were acquired for 20 min over a single 16.4-cm bed position while keeping the animal warm with a heating pad (Biograph mCT; Siemens Medical Systems). All rats fasted for at least 6 h prior to FDG PET/CT scanning, but had access to water at all times. Each rat underwent both FDG and FLT PET/CT scans on two different days (1–2 days apart).

Histological examination

Nine rats were killed and the tumors removed for histological examination within 24 h after the last PET/CT scan. The tumor was completely excised and separated from the adjacent muscle and skin. The tumors were fixed in 10% formalin for 24 h before embedding in paraffin. The blocks were cut into 5-μm sections and stained with hematoxylin and Eosin (H&E). To perform immunohistochemistry, the sections were dewaxed in Histoclear (Sigma, St. Louis, MO, USA) and rehydrated through a graded alcohol series. After antigen retrieval (Abcam, Cambridge, MA, USA), immunohistochemistry was performed in accordance with the manufacturer's protocols using the EnVision + Dual System-HRP (Dako, Glostrup, Denmark). Briefly, the sections were blocked with endogenous enzyme. The sections were incubated with the rabbit polyclonal antibody to Ki-67 (Abcam). Immunoreactivity was visualized with 3.3'-diaminobenzine, and the sections were counterstained with hematoxylin. All microscopy images were acquired using a slide scanner (3DHISTECH Ltd., Budapest, Hungary) and a microscope equipped with a spot digital camera (Nikon, Tokyo, Japan). The optical density of Ki-67-positive cells in the tumor area was determined using the MetaMorph imaging program (Molecular Device Inc., Downingtown, PA, USA). To exclude necrotic areas, corresponding sections stained with H&E were examined. The lesion with the highest density of Ki-67 was selected, and the total tumor cells and Ki-67-positive cells were counted. The Ki67 index was calculated by the fraction of Ki-67-positive samples in at least 500 tumor cells.

Data analysis

All PET/CT images were transferred to a workstation with a fusion software system (Mirada Medical, Oxford, UK) that provided multiplanar reformatted images and displayed PET images after attenuation correction, CT images, and PET/CT fusion images. The volume of interest of the tumor was delineated manually in the tumor on the basis of CT images, and the long diameter (cm) and volume

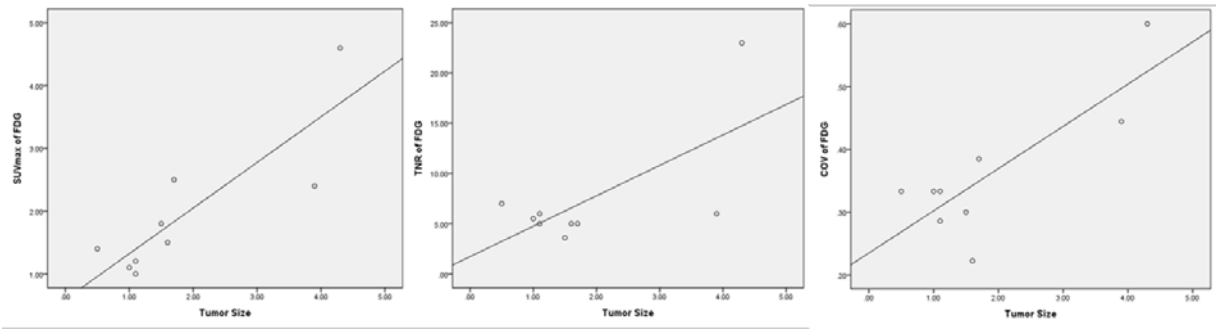

Figure 2: Correlation of SUVmax, tumor to non-tumor ratio, and coefficient of variation of FDG with tumor size.

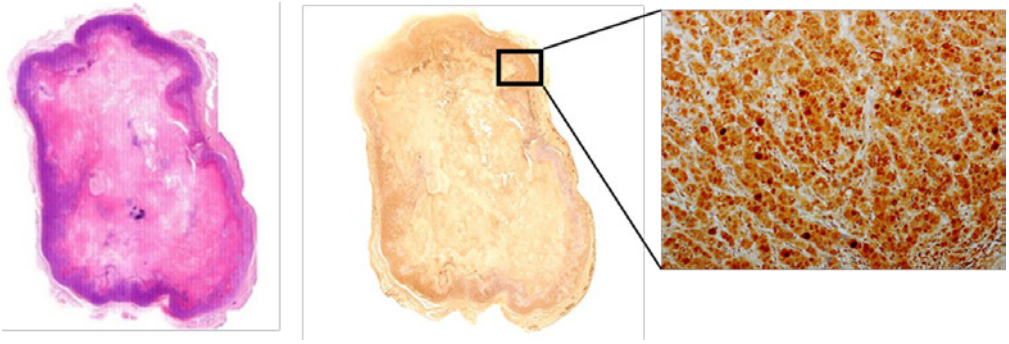

Figure 3: Hematoxylin and eosin staining and immunohistochemical expression of Ki-67. Original magnification ×400.

(cm^3) of the tumor were measured. On PET images, the highest intensity of FDG and FLT uptake within the tumor volume of interest was quantified by calculating the maximum standardized uptake value (SUVmax) and the mean standardized uptake value (SUVmean). The Tumor to Non-Tumor Ratio (TNR) was calculated with background activity of normal lung tissue using the following formula:

TNR = SUVmax of the tumor / SUVmean of the normal lung

Tumor heterogeneity was estimated using the Coefficient Of Variation (COV), defined as the standard deviation divided by the SUVmean in the delineated tumor.

Statistical analyses were performed using the Statistical Package for Social Sciences (SPSS) software (version 13.0). Pearson coefficients were used to compare SUV parameters (SUVmax, TNR, and COV) for FDG and FLT with tumor size and the amount of Ki-67 staining. Student's *t* test was used for parametric data to compare SUV parameters between FDG and FLT. Values are presented as the mean value ± standard deviation. A *P* value of <0.05 was considered statistically significant.

Results

Comparison of cellular uptake of radiotracer between FDG and FLT uptake

In total, nine tumor lesions were identified in the rats, and the average tumor size measured on CT images of PET/CT was 1.86 ± 1.32 cm. FDG uptake was clearly visualized with variable intensity in all tumors, while FLT uptake was not obvious in five tumors. FDG PET showed focal uptake in discrete regions of the tumor volume, more so than seen in the corresponding FLT PET images (Figure 1). SUVmax in FDG PET was higher than that obtained for FLT PET (1.94 ± 1.13 vs 1.00 ± 0.37, $P = 0.039$). There was no significant difference in TNR or COV between FDG PET/CT and FLT PET/CT. There were no significant correlations of SUVmax, TNR, or COV between FDG PET and FLT PET. The mean values of SUVmax, TNR, and COV are shown in Table 1.

Correlation of the radiotracer uptake with tumor size

Significant correlations of tumor size with SUVmax and TNR were seen in FDG PET imaging ($r = 0.852$, $P = 0.004$; $r = 0.676$, $P = 0.046$), but not in FLT PET imaging ($r = 0.195$, $P = 0.615$; $r = 0.419$, $P = 0.261$). A significant correlation of tumor size with COV was seen in FDG PET imaging ($r = 0.817$, $P = 0.007$), but not in FLT PET imaging ($r = 0.117$, $P = 0.764$) (Figure 2).

Histologic and immunohistochemical validation of radiotracer uptake

Ki-67 positivity ranged from 19% to 22% in all tumors. There was a significant correlation between Ki-67 and SUVmax, TNR, and COV in FLT imaging ($r = 0.866$, $P = 0.003$; $r = 0.745$, $P = 0.021$; $r = 0.721$, $P = 0.029$), but not in FDG imaging ($r = 0.478$, $P = 0.193$; $r = 0.478$, $P = 0.193$; $r = 0.617$, $P = 0.077$). As shown in Figure 3, Ki-67 staining intensity was higher in the proliferating cells of the peripheral region than in the central region.

Discussion

This study was designed to compare FDG and FLT PET imaging characteristics and differences based on tumor size in a controlled animal model. Many studies have shown that larger tumors have higher FDG uptake due to increased glucose consumption compared

Table 1: SUVmax, tumor to non-tumor ratio, and coefficient of variation in FDG and FLT.

Radiotracer	SUVmax	TNR	COV
FDG	1.94 ± 1.13	7.34 ± 5.94	0.40 ± 0.12
FLT	1.00 ± 0.37	4.11 ± 0.94	0.40 ± 0.16
P value	0.039	0.144	0.564

Data are mean ± SD.

with non-tumor tissue [5,20]. However, data on the relationship between FLT uptake and tumor size is limited. Interest in using FLT in PET imaging of malignant tumors has been increasing for several years, and this method is particularly applicable to NSCLC because of the low uptake of FLT by inflammatory cells. Many studies have shown a relationship between FDG uptake and the tumor burden [5,21,22]. The results of the present study agree with previous publications and not only show that FDG uptake is related to tumor size, but also support the idea that larger tumors have higher glucose transporter-1 expression. However, our study showed no correlations among SUVmax, TNR, and tumor size on FLT PET imaging. These results suggest that tumor growth may not be predictable based on the tumor's proliferative activity alone and that other factors, such as regional heterogeneity in cellular metabolism, may be associated with tumor growth.

Hatt et al. [23] reported that heterogeneity of FDG uptake correlated with the anatomical tumor size, with a mean COV of 0.26. Considering the spatial heterogeneity of the radiotracer within a tumor, the COV has been recognized as an important prognostic factor in colorectal cancer [24] and lung cancer [25]. Our findings are in agreement with previous studies that demonstrated that the COV of FDG uptake is closely correlated with tumor size. However, Califano et al. [26] revealed no correlation between tumor volume and FDG intratumoral heterogeneity in head and neck cancer. The assessment of tumor heterogeneity with FDG uptake is expected to play an important role in the prediction of prognosis and monitoring of therapeutic response in oncology [27]. Further studies will be required to establish the measurement method for intratumoral heterogeneity as a biomarker using FDG PET/CT.

In contrast to the analysis of tumor heterogeneity using the COV of FDG uptake, there was no statistical correlation between the FLT COV and tumor size. Presumably, lower accumulation of FLT in all tumors may result in no significant difference in COV. In addition, the microenvironment of A549 xenografts is complex, comprising minimally proliferative and hypoxic tumor cells with a large necrotic portion and non-tumorous stroma (Figure 3). Considering that differential oxygenation is another factor for a tumor's proliferative activity, we performed immunohistochemical staining for hypoxia-inducible factor-1a. However, the results of hypoxia-inducible factor-1a were not available for the statistical analysis in this study. Further experimental studies with PET/CT targeting proliferation and hypoxia using more advanced immunohistochemical stains to determine tumor characteristics are necessary to fully determine the relationship between tumor proliferation and hypoxia.

FLT, a fluorinated thymidine analogue, is trapped in the tumor cell and phosphorylated to FLT Monophosphate (FLT-MP) by thymidine kinase 1, which is a key enzyme in the DNA salvage pathway in cells [17,28]. An *in vitro* study by Rasey et al. [17] showed that FLT uptake in A549 tumor cells was strongly correlated with thymidine kinase 1 activity and an increase in the percentage of cells in the S phase. These results indicate that FLT can reflect the DNA synthesis rate and tumor cell proliferative activity. In human clinical studies, FLT uptake correlated well with the Ki-67 index in NSCLC [4]. In accordance with these previous studies, our results showed a high level of correlation among the SUVmax, TNR, FLT COV, and Ki-67 index.

However, in contrast to the strong correlation observed for FLT, the FDG SUV parameters showed no correlation with proliferative activity. *In vivo* human studies that investigated FDG PET findings in patients with NSCLC [29] and breast cancer demonstrated a strong correlation between FDG uptake and Ki-67 expression in the tumor. The discrepancies in these results could be due to the animal model used in the present study. A549 tumor cells have lower proliferative activity with more homogenous biologic features than do spontaneously occurring tumor cells. Furthermore, there was no correlation between tumor size and the Ki-67 index. These results indicate that tumor growth may be associated with multiple biological factors for aggressiveness and that growth is not only determined by proliferative activity.

The present study had several limitations in regard to the performance of PET/CT. First, we performed the human PET/CT scan in which the pixel size could be limiting factor for the assessment of tumor heterogeneity in the animal model. Second, there may be partial volume effects in small lesions, which lead to substantial uptake variation. Third, the manual segmentation had low reproducibility although repeating manual segmentation on naïve PET images by different observers would improve intra- and inter-observer variability associated manual delineation in the present study. In conclusion, FDG uptake was better visualized in tumors and correlated significantly better with tumor size compared with FLT in this NSCLC xenograft model. FDG PET tumor heterogeneity correlated well with tumor size, while no correlation was found for FLT and tumor size. FLT PET correlated well with Ki67 and tumor proliferation. Future studies should focus on repeating these comparisons in human models to determine the biological changes that affect tumor growth.

Acknowledgement

The authors wish to acknowledge the financial support of the Catholic Medical Center Research Foundation made in the program year of 2014.

References

1. Dosaka-Akita H, Hommura F, Mishina T, Ogura S, Shimizu M, Katoh H, et al. A Risk-Stratification Model of Non-Small Cell Lung Cancers Using Cyclin E, Ki-67, and ras p21 Different Roles of G1 Cyclins in Cell Proliferation and Prognosis. Cancer research. 2001; 61: 2500-2504.

2. Carlin S, Zhang H, Reese M, Ramos NN, Chen Q, Ricketts SA. A comparison

of the imaging characteristics and microregional distribution of 4 hypoxia PET tracers. Journal of Nuclear Medicine. 2014; 55: 515-521.

3. Campanile C, Arlt MJ, Kramer SD, Honer M, Gvozdenovic A, Brennecke P, et al. Characterization of different osteosarcoma phenotypes by PET imaging in preclinical animal models. Journal of nuclear medicine: official publication. Society of Nuclear Medicine. 2013; 54: 1362-1368.

4. Buck AK, Halter G, Schirrmeister H, Kotzerke J, Wurziger I, Glatting G, et al. Imaging proliferation in lung tumors with PET: 18F-FLT versus 18F-FDG. Journal of nuclear medicine: official publication. Society of Nuclear Medicine. 2003; 44: 1426-1431.

5. Xu H, Li B, Yu W, Wang H, Zhao X, Yao Y, et al. Correlation between (1)(8)F-FDG uptake and the expression of glucose transporter-1 and hypoxia-inducible factor-1alpha in transplanted VX2 tumors. Nucl Med Commun. 2013; 34: 953-958.

6. Dence CS, Ponde DE, Welch MJ, Lewis JS. Auto radiographic and small-animal PET comparisons between 18 F-FMISO, 18 F-FDG, 18 F-FLT and the hypoxic selective 64 Cu-ATSM in a rodent model of cancer. Nuclear medicine and biology. 2008; 35: 713-720.

7. Hicks RJ, Kalff V, MacManus MP, Ware RE, Hogg A, McKenzie AF, et al. (18)F-FDG PET provides high-impact and powerful prognostic stratification in staging newly diagnosed non-small cell lung cancer. Journal of nuclear medicine: official publication. Society of Nuclear Medicine. 2001; 42: 1596-1604.

8. de Geus-Oei LF, van der Heijden HF, Corstens FH, Oyen WJ. Predictive and prognostic value of FDG-PET in nonsmall-cell lung cancer. Cancer. 2007; 110: 1654-1664.

9. Vansteenkiste JF, Stroobants SG, De Leyn PR, Dupont PJ, Verbeken EK. Potential use of FDG-PET scan after induction chemotherapy in surgically staged IIIa-N2 non-small-cell lung cancer: a prospective pilot study. The Leuven Lung Cancer Group. Annals of oncology. 1998; 9: 1193-1198.

10. Krohn KA, Mankoff DA, Eary JF. Imaging Cellular Proliferation as a Measure of Response to Therapy. The Journal of Clinical Pharmacology. 2001; 41: 96-103.

11. Vander Borght T, Labar D, Pauwels S, Lambotte L. Production of [2-11C] thymidine for quantification of cellular proliferation with PET. International Journal of Radiation Applications and Instrumentation. Part A. Applied Radiation and Isotopes. 1991; 42: 103-104.

12. Yamamoto Y, Nishiyama Y, Kimura N, Ishikawa S, Okuda M, Bandoh S, et al. Comparison of 18F-FLT PET and 18F-FDG PET for preoperative staging in non-small cell lung cancer. European journal of nuclear medicine and molecular imaging. 2008; 35: 236-245.

13. Hui W, Jinming Z, Jiahe T, Baolin Q, Tianran L, Yingmao C, et al. Using Dual-Tracer PET to Predict the Biologic Behavior of Human Colorectal Cancer. Journal of Nuclear Medicine. 2009; 50: 1857-1864.

14. van Waarde A, Cobben DC, Suurmeijer AJ, Maas B, Vaalburg W, de Vries EF, et al. Selectivity of 18F-FLT and 18F-FDG for differentiating tumor from inflammation in a rodent model. Journal of nuclear medicine: official publication. Society of Nuclear Medicine. 2004; 45: 695-700.

15. Mudd S, Holich K, Voorbach M, Cole T, Reuter D, Tapang P, et al. Pharmacodynamic evaluation of irinotecan therapy by FDG and FLT PET/CT imaging in a colorectal cancer xenograft model. Molecular Imaging and Biology. 2012; 14: 617-624.

16. Buck AK, Hetzel M, Schirrmeister H, Halter G, Möller P, Kratochwil C, et al. Clinical relevance of imaging proliferative activity in lung nodules. European journal of nuclear medicine and molecular imaging. 2005; 32: 525-533.

17. Rasey JS, Grierson JR, Wiens LW, Kolb PD, Schwartz JL. Validation of FLT Uptake as a Measure of Thymidine Kinase-1 Activity in A549 Carcinoma Cells. Journal of Nuclear Medicine. 2002; 43: 1210-1217.

18. Gerlinger M, Rowan AJ, Horswell S, Larkin J, Endesfelder D, Gronroos E, et al. Intratumor heterogeneity and branched evolution revealed by multiregion sequencing. The New England journal of medicine. 2012; 366: 883-892.

19. Davnall F, Yip CS, Ljungqvist G, Selmi M, Ng F, Sanghera B, et al. Assessment of tumor heterogeneity: an emerging imaging tool for clinical practice? Insights into imaging. 2012; 3: 573-589.

20. Heudel P, Cimarelli S, Montella A, Bouteille C, Mognetti T. Value of PET-FDG in primary breast cancer based on histopathological and immunohistochemical prognostic factors. Int J Clin Oncol. 2010; 15: 588-593.

21. Izuishi K, Yamamoto Y, Sano T, Takebayashi R, Masaki T, Suzuki Y. Impact of 18-fluorodeoxyglucose positron emission tomography on the management of pancreatic cancer. Journal of Gastrointestinal Surgery. 2010; 14: 1151-1158.

22. Hatt M, Cheze-le Rest C, van Baardwijk A, Lambin P, Pradier O, Visvikis D. Impact of tumor size and tracer uptake heterogeneity in (18)F-FDG PET and CT non-small cell lung cancer tumor delineation. Journal of nuclear medicine: official publication. Society of Nuclear Medicine. 2011; 52: 1690-1697.

23. Bundschuh RA, Dinges J, Neumann L, Seyfried M, Zsoter N, Papp L, et al. Textural Parameters of Tumor Heterogeneity in 18F-FDG PET/CT for Therapy Response Assessment and Prognosis in Patients with Locally Advanced Rectal Cancer. Journal of Nuclear Medicine. 2014; 55: 891-897.

24. Ganeshan B, Panayiotou E, Burnand K, Dizdarevic S, Miles K. Tumour heterogeneity in non-small cell lung carcinoma assessed by CT texture analysis: a potential marker of survival. European radiology. 2012; 22: 796-802.

25. Califano JA, Nakajima EC, Laymon C, Oborski M, Hou W, Wang L, et al. Quantifying Metabolic Heterogeneity in Head and Neck Tumors in Real Time: 2-DG Uptake Is Highest in Hypoxic Tumor Regions. PLoS ONE. 2014; 9: 102452.

26. Tixier F, Le Rest CC, Hatt M, Albarghach N, Pradier O, Metges J-P, et al. Intratumor heterogeneity characterized by textural features on baseline 18F-FDG PET images predicts response to concomitant radiochemotherapy in esophageal cancer. Journal of Nuclear Medicine. 2011; 52: 369-378.

27. Eriksson S, Kierdaszuk B, Munch-Petersen B, Oberg B, Johansson NG. Comparison of the substrate specificities of human thymidine kinase 1 and 2 and deoxycytidine kinase toward antiviral and cytostatic nucleoside analogs. Biochemical and biophysical research communications. 1991; 176: 586-592.

28. Vesselle H, Schmidt RA, Pugsley JM, Li M, Kohlmyer SG, Vallières E, et al. Lung cancer proliferation correlates with [F-18] fluorodeoxyglucose uptake by positron emission tomography. Clinical Cancer Research. 2000; 6: 3837-3844.

29. Avril N, Menzel M, Dose J, Schelling M, Weber W, Janicke F, et al. Glucose metabolism of breast cancer assessed by 18F-FDG PET: histologic and immunohistochemical tissue analysis. Journal of nuclear medicine: official publication. Society of Nuclear Medicine. 2001; 42: 9-16.

Austin J Radiol - Volume 3 Issue 4 - 2016
ISSN : 2473-0637 | www.austinpublishinggroup.com

Citation: Choi EK, Jung HY, Yoo IR, Chung YA, Park SI and Maeng LS. Comparison of FDG and FLT PET/CT Imaging Based on Human Non-Small Cell Lung Carcinoma Tumor Size in a Small Animal Model. Austin J Radiol. 2016; 3(4): 1058.